Near-optimal polynomial interpolation on spherical triangles *

A. Sommariva and M. Vianello [1]
University of Padova, Italy

March 20, 2021

2010 AMS subject classification: Primary 41A10, 65D05.

Keywords: spherical triangles, trigonometric polynomials, spherical polynomials, Dubiner distance, Chebyshev norming grids, Fekete-like points, polynomial interpolation.

Abstract

By the fundamental notion of Dubiner distance on a compact set, we construct Chebyshev polynomial norming grids in the sup-norm on spherical triangles. These grids can be used to extract Fekete-like interpolation points with slowly increasing Lebesgue constant.

1 Introduction

The goal of this paper is to construct "good" discretizations of spherical triangles, that could allow to extract suitable interpolation points for polynomial interpolation, namely unisolvent point sets with slowly increasing Lebesgue constant. Indeed, the subject of *global interpolation by spherical polynomials* seems to have been overlooked with respect to other approaches in the approximation literature on spherical triangles (despite their relevance for example in the field of geomathematical modelling), and also with respect to other well-studied regions such as the whole sphere and lat-long rectangles; cf., e.g., [1, 2, 9, 10, 14, 15, 19, 27] with the references therein.

To this purpose, we adopt the relevant notion of *Dubiner distance* on compact sets, which is intimately related to polynomial and trigonometric approximation. Moreover, we strongly rely on polynomial inequalities and in particular on the other relevant notion of *norming set* for a polynomial space. Finally, we resort

*Work partially supported by the DOR funds and the biennial project BIRD 192932 of the University of Padova, and by the INdAM-GNCS. This research has been accomplished within the RITA "Research ITalian network on Approximation" and the UMI Group TAA "Approximation Theory and Applications".

[1]Corresponding author: marcov@math.unipd.it

to some algorithms devoted to the computation of *Approximate Fekete Points* for polynomial interpolation starting from norming sets, developed in the last decade after [20] and here adapted to spherical polynomials. For an overview of this concepts and methods, we may quote e.g. [6, 4, 8].

We begin by recalling that the Dubiner distance on a compact unidimensional or multidimensional set K, say $dub(x,y) = dub_K(x,y)$, $x, y \in K$, is defined as

$$dub(x,y) = \sup_{deg(p)\geq 1,\, \|p\|_K \leq 1} \left\{ \frac{1}{deg(p)} \, |\arccos(p(x)) - \arccos(p(y))| \right\} . \qquad (1)$$

Originally intriduced in the seminal paper [13] for $K \subset \mathbb{R}^d$ with p varying in the space of algebraic polynomials restricted to K, it has been later extended to trigonometric polynomials on subintervals of the period, i.e. on $K = [-\omega, \omega]$ with $0 < \omega \leq \pi$ (cf. [25]).

It is simple to check that in the algebraic case the Dubiner distance is invariant under invertible affine transformations, whereas in the trigonometric case it is invariant under interval translations. A basic property, that comes directly from the definition, is that it is monotone *nonincreasing with respect to set inclusion*, namely

$$\text{if } \; x, y \in K \subseteq H \;\; \text{ then } \;\; dub_H(x,y) \leq dub_K(x,y) \, . \qquad (2)$$

The notion of Dubiner distance plays a deep role in multivariate polynomial approximation, cf. e.g. [6, 13]. Unfortunately, such a distance is explicitly known only in the univariate case on intervals (where it is the *arccos* distance by the Van der Corput-Schaake inequality), and on cube, simplex, sphere and ball (in any dimension), cf. [6]. On the other hand, it can be often estimated, for example on smooth convex bodies via a tangential Markov inequality on the boundary, or on starlike polygons; cf. [17, 26].

Recently in [25], the trigonometric Dubiner distance has been computed analytically via Szegö variant of Videnskii inequality, obtaining the explicit formula

$$dub(\theta, \phi) = 2\,|F_\omega(\theta) - F_\omega(\phi)| \;\; , \;\; \theta, \phi \in [-\omega, \omega] \, , \qquad (3)$$

where

$$F_\omega(\theta) = 2 \arcsin\left(\frac{\sin(\theta/2)}{\sin(\omega/2)} \right) .$$

Its connection with the theory of norming sets for both algebraic and trigonometric polynomial spaces is given by the following elementary but powerful lemma, proved in [3].

Lemma 1 *Let X be a compact subset of a compact set $K \subset \mathbb{R}^d$ (or of $K = [-\omega, \omega]$ in the univariate trigonometric case), whose covering radius $R_{dub}(X)$ with respect to the Dubiner distance does not exceed θ/n, where $\theta \in (0, \pi/2)$ and $n \geq 1$, i.e.*

$$R_{dub}(X) = \max_{x\in K} dub(x, X) = \max_{x\in K} \min_{y\in X} dub(x,y) \leq \frac{\theta}{n} \, . \qquad (4)$$

Then, the following inequality holds

$$\|p\|_K \leq \frac{1}{\cos\theta}\,\|p\|_X\ ,\quad \forall p \in \mathbb{P}_n^d(K)\ \ (or\ \ \forall p \in \mathbb{T}_n(K))\ . \tag{5}$$

2 Dubiner distance and norming grids

Let us now focus on a spherical triangle of the unit sphere with vertices U, V, W, say $\mathcal{T} = U\widehat{V}W$, contained in a hemisphere. The key observation in this context is that

- **Remark 1**: *a trivariate polynomial restricted to a great circle arc of length* 2ω *is (by a suitable change of variables) a trigonometric polynomial of the same degree on* $[-\omega, \omega]$.

Our goal is to construct a Chebyshev-like rectilinear grid on the planar triangle UVW with grid points say $G = \{P_{ij}\}$, whose radial projection on $\mathcal{T}$ is a curvilinear grid made by great circle arcs, and to estimate the Dubiner covering radius $R_{dub_{\mathcal{T}}}(\widehat{G})$ of the corresponding grid points, $\widehat{G} = \{P_{ij}/\|P_{ij}\|_2\}$; see Fig. 1. Unfortunately, to our knowledge the Dubiner distance of a spherical triangle is not known analytically. However, as we shall see below it can be estimated via the Dubiner distance on great circle arcs, which is nothing but the trigonometric Dubiner distance (3).

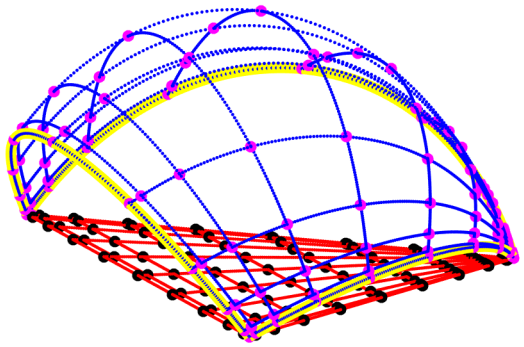

Figure 1: Radially mapped Chebyshev-Lobatto grid from the planar supporting triangle to a spherical triangle.

To this purpose, first we observe that any segment $[P, Q]$ in the supporting

planar triangle UVW is radially projected onto a geodesic arc of the spherical triangle, *thus determining a sector of the corresponding great disk*.

Consider now the spherical cap circumscribing the spherical triangle (whose base is the circumcircle of the supporting planar triangle). *The (acute) angle, say γ, between $[P, Q]$ and the arc chord* (the segment joining the arc extrema), that is also the angle between the line determined by such a chord and the triangle plane, *cannot exceed the angle between the cap and its tangent planes at the base circle, that coincides with the cap half angle, say $\omega^* > 0$*, as it can be easily seen (this angle is the base circle "colatitude" thinking to a polar cap).

Indeed, see Fig. 2, concerning a great disk with the segment $[P, Q]$ radially projected onto the geodesic arc $\widehat{AB}$: the angle between $[A, B]$ and $[P, Q]$, that is $\widehat{Q'AB}$ since $[A, Q']$ is parallel to $[P, Q]$, cannot exceed the angle between the tangent line at W and the segment $[W, E]$ (a diameter of the base circle of the cap circumscribing the spherical triangle). The latter angle coincides with the cap half angle $\widehat{WON}$, since both are complementary to $\widehat{OWE}$.

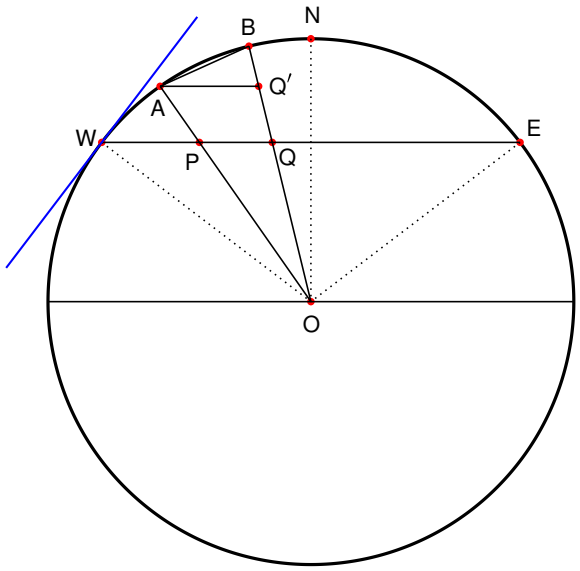

Figure 2: Great disk corresponding to the great circle of the sphere where a segment $[P, Q]$ in the planar triangle is radially projected; $\widehat{WE}$ is the section of the cap circumscribing the spherical triangle.

2.1 Geometric and numerical study

Now, let us consider a sector as just described, by no loss of generality we can think to a sector of the unit circle with angles in $[-\omega, \omega]$. Let $\mathcal{C}_m = \{t_j = t_j(m) = 0.5\cos(j\pi/m) + 0.5\,,\ 0 \le j \le m\}$ be the $m+1$ Chebyshev-Lobatto nodes in $[0,1]$,

$$\mathcal{C}_m(P,Q) = \{P_j = (u(t_j), v(t_j)) = t_j P + (1-t_j)Q\,,\ 0 \le j \le m\}\ ,\quad t_j \in \mathcal{C}_m \quad (6)$$

the Chebyshev-Lobatto nodes of $[P,Q]$, and

$$\Theta_m = \Theta_m(\omega; P, Q) = \{\theta_j = \theta(t_j) = \arctan\left(v(t_j)/u(t_j)\right),\ 0 \le j \le m\} \quad (7)$$

the corresponding radially projected $m+1$ angles in $[-\omega, \omega]$; see Fig. 3. By *Thales Theorem* on intercepts (cf. [24]) the set Θ_m is the same for any segment parallel to $[P,Q]$ joining the sector straight sides, in particular for the parallel segment with an extremum coinciding with the nearest arc extremum, see the segment $[A, Q']$ parallel to $[P,Q]$ in Fig. 3.

Hence, we can compute the trigonometric Dubiner covering radius $R_{dub}(\Theta_m)$ on segments of the form

$$[P,Q] = [A(\omega), sB(\omega)]\ ,\quad s \in (0,1]\ , \quad (8)$$

where $A(\omega) = (\cos(\omega), \sin(\omega))$, $B(\omega) = (\cos(\omega), -\sin(\omega))$. Notice that here

$$u(t) = \cos(\omega)(t + (1-t)s)\ ,\quad v(t) = \sin(\omega)(t - (1-t)s)\ ,$$

and hence by easy computations

$$\partial_t \theta = \partial_t \arctan\left(\tan(\omega)\,\frac{t-(1-t)s}{t+(1-t)s}\right)$$

$$= \frac{2s\tan(\omega)}{(t+(1-t)s)^2 + \tan^2(\omega)(t-(1-t)s)^2}\ > 0\ . \quad (9)$$

Then $\theta_j = \theta(t_j) > \theta_{j+1} = \theta(t_{j+1})$ since $t_j > t_{j+1}$ and recalling that the function $F_\omega(\theta)$ in (3) is increasing in θ, the trigonometric Dubiner distance between two consecutive radial Chebyshev-like angles is $dub(\theta_j, \theta_{j+1}) = 2(F_\omega(\theta_j) - F_\omega(\theta_{j+1}))$. On the other hand, if $\theta \in [\theta_j, \theta_{j+1}]$ then $dub(\theta_j, \theta_{j+1}) = dub(\theta_j, \theta) + dub(\theta, \theta_{j+1})$, so that the covering radius of the point set $\Theta_m(\omega, A(\omega), sB(\omega))$ is half the maximal Dubiner distance between consecutive nodes, that is the trivariate function

$$\mathcal{R}(m,\omega,s) = R_{dub}(\Theta_m(\omega, A(\omega), sB(\omega))) = \frac{1}{2}\max_{0\le j\le m-1} dub(\theta_j, \theta_{j+1})$$

$$= \max_{0\le j\le m-1}(F_\omega(\theta_j) - F_\omega(\theta_{j+1}))\ . \quad (10)$$

The analytical study of $\mathcal{R}$ turns out to be an extremely hard task, because it would require locating the discrete node interval where the maximal value is attained. Nevertheless, an extensive numerical study is possible.

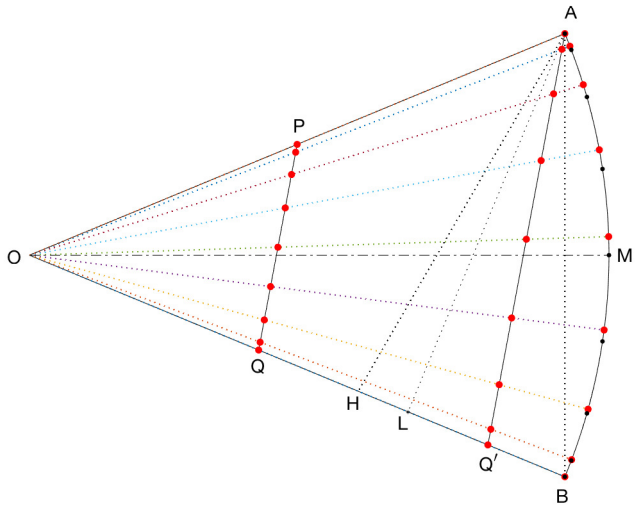

Figure 3: $m+1=9$ radially mapped Chebyshev-Lobatto nodes $\mathcal{C}_m(A,Q')$ from the segment $[A,Q']$parallel to $[P,Q]$ to the arc with $\omega=\pi/8$ (red dots), together with the set (12) of equispaced points in the Dubiner distance (black dots). Notice that $Q'\in(H,B]$, where H is such that $\widehat{BAH}=\omega^*=\pi/6$.

First, we determine a lower bound for s, in order to keep the function $\mathcal{R}$ uniformly $\mathcal{O}(1/m)$ in (ω,s), on every geodesic arc obtained by radial projection of any segment $[P,Q]$ in the supporting planar triangle of any possible spherical triangle circumscribed by a cap with half angle ω^*. By construction, if the length of such an arc is 2ω then $0<\omega\leq\omega^*$, since the arc lies on the cap.

On the other hand, as already observed, the angle γ between $[P,Q]$ and the arc chord is such that $\gamma\leq\omega^*$, and clearly we have also $\gamma<\pi/2-\omega$. Now, by imposing the constraint $\omega^*<\pi/2-\omega$, we get $0<\omega\leq\omega^*<\pi/2-\omega$, which gives $\omega<\pi/4$ and thus $\omega^*=\max\omega<\pi/4$. Geometrically, we see in Fig. 3 that this construction corresponds to $\sigma(\omega,\omega^*)\leq s\leq 1$ where

$$\sigma(\omega,\omega^*)=1-2\sin^2(\omega)-2\sin(\omega)\cos(\omega)\tan(\omega^*-\omega)\ . \tag{11}$$

In fact, let the angle $\widehat{BAH}$ be equal to ω^*, and let us term L the orthogonal projection of A on the opposite sector straight side. Then the angle $\widehat{BAL}$ is equal to ω being complementary to $\widehat{LBA}$, that in turn is complementary to $\widehat{BOM}=\omega$, and hence $|L-B|=|A-B|\sin(\omega)=2\sin^2(\omega)$. On the other hand, the angle $\widehat{LAH}$ equals $\omega^*-\omega$ and thus $|H-L|=|A-L|\tan(\omega^*-\omega)=2\sin(\omega)\cos(\omega)\tan(\omega^*-\omega)$, i.e. $|H-B|=1-\sigma(\omega,\omega^*)=2\sin^2(\omega)+2\sin(\omega)\cos(\omega)\tan(\omega^*-\omega)$.

We have numerical evidence that the angles $\theta_j\in\Theta_m(\omega,A(\omega),sB(\omega))$ are nearly equispaced in the trigonometric Dubiner distance on $[-\omega,\omega]$, with spacing

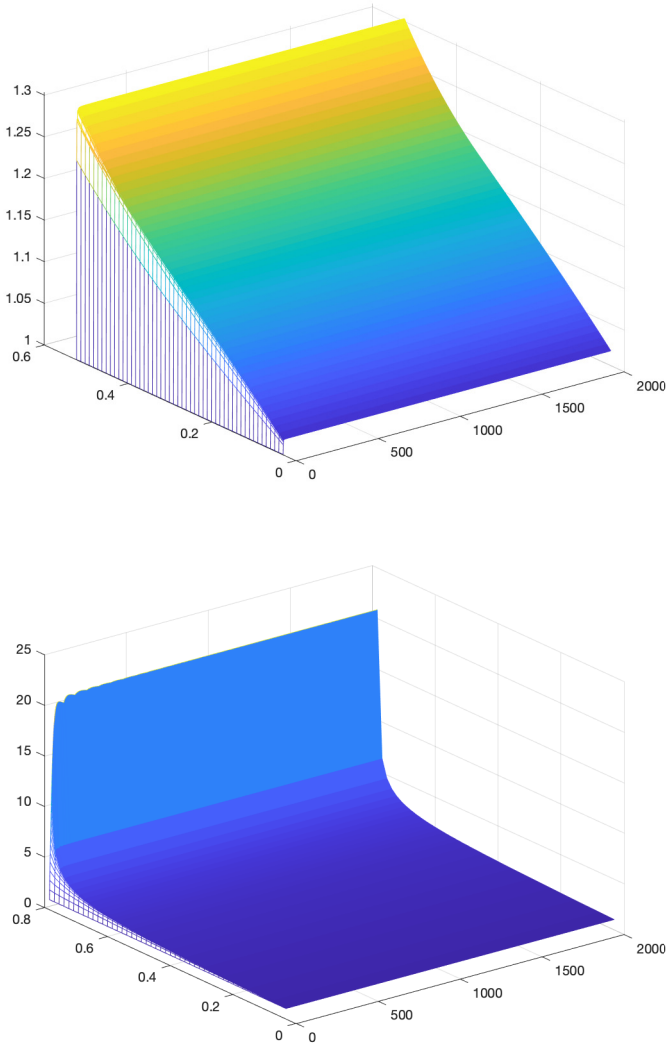

Figure 4: The maximal ratio $\max_{s\in[\sigma(\omega,\omega^*),1]} \mathcal{R}(m,\omega,s))/(\pi/m)$ for $m = 1,\dots,2000$ and $\omega \in [\pi/100,\omega^*]$ with $\omega^* = \pi/6$ (top) and $\omega^* = 0.999\,\pi/4$ (bottom).

$\approx 2\pi/m$ and thus

$$\mathcal{R}(m,\omega,s) \approx \pi/m\ ,\quad \omega \in (0,\omega^*]\ ,\quad s \in [\sigma(\omega,\omega^*),1]\ ,$$

if ω is not too close to $\pi/4$, whereas the ratio $\mathcal{R}(m,\omega,s)/(\pi/m)$ increases rapidly as ω can approach $\pi/4$; see Fig. 4. In Fig. 3 we have also plotted for comparison

(asterisks) another set of Chebyshev-like nodes on the arc that are known to be exactly equispaced in the trigonometric Dubiner distance (as it can be easily checked, cf. [25]), namely

$$\phi_j = 2\arcsin(t_j \sin(\omega/2)) \ , \quad 0 \le j \le m \ . \tag{12}$$

Now, since it is clear by the geometric construction that the standard distance $|\Delta\theta_j|$ between consecutive angles close to $-\omega$ increases as s decreases from 1 to σ, and $dub(\theta_j, \theta_{j+1}) > |\arccos(\theta_j) - \arccos(\theta_{j+1})| > |\Delta\theta_j|$ (cf. (3)), one could think that the same happens also to the Dubiner distance. However, we have numerical evidence that this is not true in general.

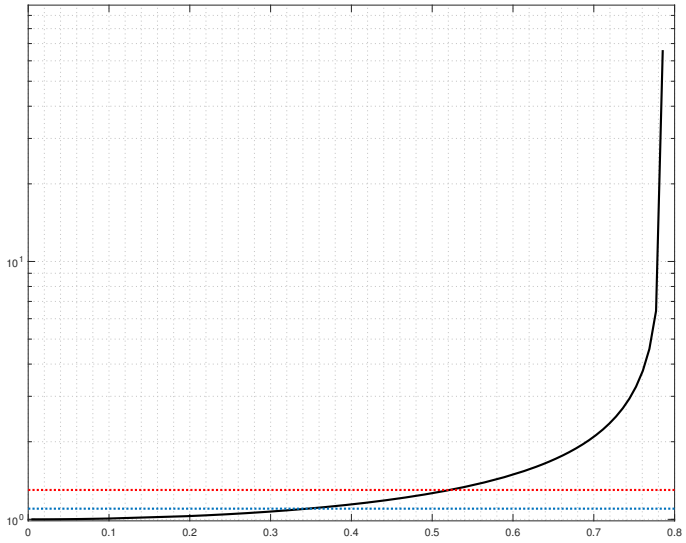

Figure 5: The function $\alpha(\omega^*)$ for $\omega^* \in (0, 0.9999\,\pi/4]$; the horizontal lines are $y = 1.1$ and $y = 1.3$ (log scale).

The maximal ratio $\max_{s\in[\sigma(\omega,\omega^*),1]} \mathcal{R}(m,\omega,s))/(\pi/m)$ is plotted in Fig. 3 for two values of ω^* and $m = 1, \ldots, 2000$. Observe that it appears an increasing function of ω for fixed m and ω^*. On the base of extensive numerical computations, we may then estabilish the following

- **Conjecture**:

$$\max_{\omega\in(0,\omega^*],\, s\in[\sigma(\omega,\omega^*),1]} \mathcal{R}(m,\omega,s) \le \alpha(\omega^*)\frac{\pi}{m} \ , \quad \forall m \ge 1 \ ,$$

$$\alpha(\omega^*) = \sup_{m\ge 1} \max_{s\in[1-\sin^2(\omega^*),1]} \frac{\mathcal{R}(m,\omega^*,s)}{\pi/m} \ , \tag{13}$$

where $\alpha(\omega^*) > 1$ is an increasing function of $\omega^* \in (0, \pi/4)$.

A plot of $\alpha(\omega^*)$ is given in Fig. 5, corresponding to a fine discretization in ω, ω^* and m up to 10^4 (the latter being far beyond any reasonable need in the interpolation framework of the present paper). The values of $\alpha(\omega^*)$ remain close to 1 up to a neighborhood of $\pi/4$ where they increase rapidly: for example, $\alpha(\pi/8) \approx 1.1$, $\alpha(\pi/6) \approx 1.3$, $\alpha(\pi/5) \approx 1.6$, $\alpha(0.9\,\pi/4) \approx 2.2$, whereas $\alpha(0.999\,\pi/4) \approx 20.9$, $\alpha(0.9999\,\pi/4) \approx 59.2$.

We observe that a choice like for example $\max \omega^* = \pi/5$ to stay bounded away from $\pi/4$ is not really restrictive, since norming grids can be constructed by finite union and any spherical triangle can be easily iteratively subdivided into smaller triangles, for example via the midpoints of the sides.

2.2 Chebyshev-Dubiner norming grids

We are now ready to estimate the covering radius of a radially mapped Chebyshev grid like that in Fig. 1 with respect to the Dubiner distance on a spherical triangle $\mathcal{T} = U\widehat{V}W$.

The first observation is that if we take $m+1$ Chebyshev-Lobatto nodes on each side of the planar triangle UVW and connect by lines one vertex to the nodes of the opposite side, say U to $[V, W]$, and one to the other the nodes with the same index of the other two sides $[U, V]$ and $[U, W]$, we obtain a trapezoidal grid like that of Fig. 1 (see also Fig. 6). The relevant fact is that

- **Remark 2**: *the grid points of any grid segment are exactly the Chebyshev-Lobatto nodes of that segment, by Thales Theorem on intercepts, which again plays a key role in the whole construction. In particular, the grid segments connecting $[U, V]$ to $[U, W]$ are parallel. More, if we take any point P in the triangle, then the line through U and P, which intersects $[V, W]$ at a point P', intersects such parallel segments exactly at the Chebyshev nodes of $[U, P']$; see Fig. 6.*

We may call $G_m = \{P_{ij}\}$ such a grid, which has cardinality $card(G_m) = 1 + (m+1)m = m^2 + m + 1$. Grids of this type have been proved to be norming sets in the sup-norm for total degree polynomials on planar triangles, cf. e.g. [7]. Concerning spherical triangles, we can prove the following Proposition. In the sequel, we shall denote by $\mathbb{P}_n(S^2) = \mathbb{P}_n^3(S^2)$ the spherical polynomials of degree not exceeding n, where $dim(\mathbb{P}_n(S^2)) = (n+1)^2$, and by $\|f\|_K$ the sup-norm of a continuous function on the continuous or discrete compact set $K \subseteq S^2$.

Proposition 1 *Assume that Conjecture (13) holds. Let $\mathcal{T} = U\widehat{V}W$ be a spherical triangle whose circumscribing cap has angle $2\omega^* < \pi/2$. Consider the Chebyshev-Lobatto rectilinear grid $G_m = \{P_{ij}\} \subset UVW$ described above, corresponding to $m+1$ nodes on each grid segment (cf. Fig. 6).*

Then the covering radius of the radially mapped curvilinear grid $\widehat{G}_m = \{P_{ij}/\|P_{ij}\|_2\}$ with respect to the Dubiner distance on $\mathcal{T}$, that we call Chebyshev-Dubiner grid, can be estimated as

$$R_{dub}(\widehat{G}_m) \leq \alpha(\omega^*)\frac{2\pi}{m}\,, \quad \forall m \geq 1\,. \tag{14}$$

Moreover, if $m = kn$ with $n \geq 1$ and $k > 4\alpha(\omega^*)$, then $\widehat{G}_{kn}$ is a norming set in the sup-norm for $\mathbb{P}_n(\mathcal{T})$, since the following inequality holds

$$\|p\|_{\mathcal{T}} \leq c_k(\omega^*) \, \|p\|_{\widehat{G}_{kn}} \ , \quad \forall p \in \mathbb{P}_n(S^2) \ , \quad c_k(\omega^*) = \frac{1}{\cos\left(\frac{2\pi\alpha(\omega^*)}{k}\right)} \ . \tag{15}$$

Proof. Let $\mathscr{P} = P/\|P\|_2$ a point on the spherical triangle, where P its unique preimage on the planar triangle (the radial projection of the planar into the spherical triangle being one-to-one). We can assume with no loss of generality that the situation is that depicted in Figure 6. The point $\mathscr{P}$ lies in a curvilinear geodesic quadrangle (possibly degenerating into a triangle at U), whose vertices are determined by the four vertices of the trapezium (triangle) containing P.

In order to estimate the Dubiner distance of $\mathscr{P}$ from the vertices, we can move in the planar triangle along the segment $[U, P']$ from P to one of the trapezium bases, up to the intersection point such that the Dubiner distance measured along the geodesic arc connecting $U/\|U\|_2$ with $P'/\|P'\|_2$ is minimum. Since the intersection points with the trapezium bases are Chebyshev-Lobatto nodes of $[U, P']$ (see Remark 2), by Conjecture (13) such Dubiner distance cannot exceed $\alpha(\omega^*)\,\pi/m$, and the same holds true for the Dubiner distance on $\mathcal{T}$ by the set monotonicity property (2).

Now, we can make the same reasoning along the relevant trapezium base, obtaining that the Dubiner distance of $\mathscr{P}$ from the nearest vertex of its curvilinear quadrangle cannot exceed the sum of distances by the metric triangle inequality, that is $\alpha(\omega^*)\,\pi/m + \alpha(\omega^*)\,\pi/m = 2\alpha(\omega^*)\,\pi/m$.

Moreover, if $m = kn$ with $n \geq 1$ and $k > 4\alpha(\omega^*)$, then $R_{dub}(\widehat{G}_m) \leq \theta/n$ with $\theta = 2\pi\alpha(\omega^*)/k < \pi/2$ and by Lemma 1 the polynomial inequality (15) follows. $\square$

Remark 3 One could ask why not using the angles (12) for the whole construction, in view of the fact that they are exactly equispaced in the trigonometric Dubiner distance. However, they are not suitable to our purposes since for a given arc the corresponding points on the chord $[A(\omega), B(\omega)]$ are a nonlinear transformation of the Chebyshev-Lobatto nodes, whereas as we have seen above we need an affine transformation of such nodes to obtain a triangle grid, in view of Thales Theorem on intercepts.

Remark 4 A similar construction and analysis, that we omit for brevity, can be carried out starting from m Chebyshev nodes in $(-1, 1)$, i.e. the zeros of $T_m(t) = \cos(m \arccos(t))$. In this case, a conjecture exactly like (13) can be estabilished, where the relevant function $\alpha(\omega^*)$ has essentially the same behavior, and a curvilinear norming grid as in (15) can be constructed with all interior nodes and cardinality $(m+1)^2$.

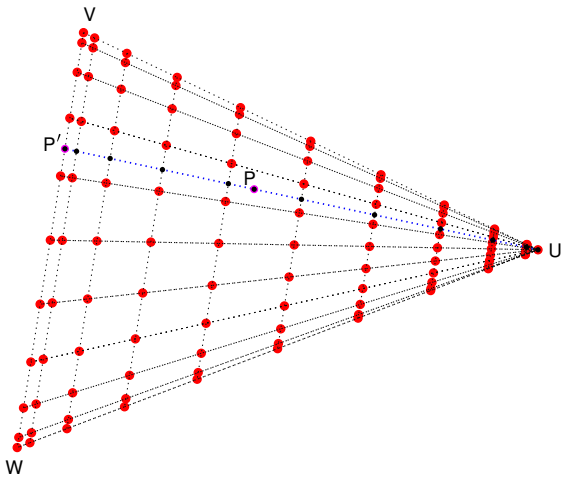

Figure 6: Chebyshev-Lobatto grid with $m = 10$ on the planar supporting triangle of a spherical triangle $\mathcal{T} = U\widehat{V}W$, cf. Fig. 1.

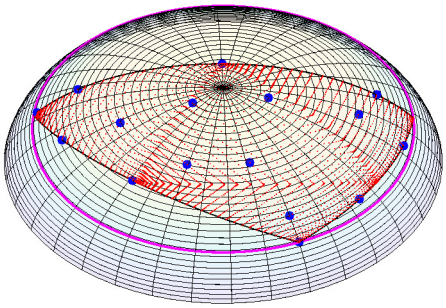

Figure 7: $(n+1)^2 = 16$ Approximate Fekete Points for interpolation degree $n = 3$ extracted from the union of Chebyshev-Lobatto grids of a splitted spherical triangle.

3 Fekete-like interpolation

Multivariate polynomial inequalities of the form (15), i.e.

$$\|p\|_K \leq c\,\|p\|_{X_n}\ ,\ \ \forall p \in \mathbb{P}_n^d(K)\ , \tag{16}$$

where X_n is a finite set of a compact set or manifold $K \subset \mathbb{R}^d$ and c is a constant have been studied extensively, from both the theoretical and the computational point of view, especially after the seminal paper [8]. The norming sets sequence $\{X_n\}$ is known as "admissible mesh" or "polynomial mesh" in the approximation literature if

$$card(X_n) = \mathcal{O}(N^\beta)\ ,\ \ \beta \geq 1\ ,\ \ N = N_n(K) = dim(\mathbb{P}_n^d(K))\ , \tag{17}$$

and are termed "optimal" when $\beta = 1$ (since necessarily $card(X_n) \geq N$); cf., e.g., [4, 7, 16, 17] and the references therein.

Relevant properties are that polynomial meshes are preserved by affine transformations and can be constructed by finite union/product and by algebraic transformations. Their relationship with the Dubiner distance (exploited in Proposition 1) is manifest in Lemma 1 of Section 1.

In the polynomial interpolation framework, polynomial meshes are very useful due to the following elementary property: the Fekete points (that are points maximing the absolute value of the Vandermonde determinant) extracted from a polynomial mesh have a Lebesgue constant (the uniform norm of the interpolation operator) bounded as

$$\Lambda(X_n) \leq c\,N\ , \tag{18}$$

i.e. growing at most linearly in the polynomial space dimension and thus at most polynomially in the degree; [8]. Bound (18) has to be compared with the theoretical bound of the Fekete points of K, namely $\Lambda(K) \leq N$.

Unfortunately, the "continuous" Fekete points are known only in very few instances, and their computation is an extremely difficult large scale optimization problem. The situation could appear better with the Fekete points of a polynomial mesh, however their computation is known to be a NP-hard optimization problem, since it is ultimately equivalent to the extraction of a "maximum volume" square submatrix from a rectangular Vandermonde matrix (cf. [11]).

Consequently, one should adopt heuristic or stochastic approaches. Indeed, one of the successful methods is given by the following greedy algorithm, originally proposed in [20]. Let $\{p_j\}$, $1 \leq j \leq N$ be a fixed basis of $\mathbb{P}_n^d(K)$, $X_n = \{\xi_i\}$, $1 \leq i \leq M$, $M > N$, a polynomial mesh of K, and

$$V = (v_{ij}) = (p_j(\xi_i)) \in \mathbb{R}^{M \times N}$$

the corresponding rectangular Vandermonde-like matrix, which is full-rank in view of (16). The extraction algorithm of what are called the Approximate Fekete Points $\tilde{\mathcal{F}}_n \subset X_n$ is briefly sketched below. For a comprehensive discussion on Fekete-like discrete extremal sets, algorithmic details, examples and numerical tests on different compact sets we refer the reader, e.g., to [4, 5].

- **Algorithm AFP** (Approximate Fekete Points)

(1) $V = QR$, with $Q \in \mathbb{R}^{M\times N}$ orthogonal, $R \in \mathbb{R}^{N\times N}$ triangular nonsingular

(2) $W = Q^t$
`for` $k = 1, \dots, N$
• select the largest norm column $col_{i_k}(W)$
• subtract from every column of W its orthogonal projection onto col_{i_k}
`end`

(3) $\tilde{\mathcal{F}}_n = \{\xi_{i_1}, \dots, \xi_{i_N}\}$

Some comments are now in order. Step (1) is useful to reduce the conditioning of the matrix V, by the change of polynomial basis to a discrete orthonormal one $(q_1, \dots, q_N) = (p_1, \dots, p_N)\, R^{-1}$, so that $Q = (q_j(\xi_i))$. On the other hand, Step (2) can be implemented by solving the underdetermined moment system $Q^t u = b$ for any nonzero vector b, by QR factorization with column pivoting of Q^t: in Matlab this can be done automatically by applying the backslash operator, $u = Q^*\backslash b$. The resulting sparse vector sparse has N nonzero elements, whose indexes $\{i_1, \dots, i_N\}$ determine the Approximate Fekete Points.

It is worth stressing that, though Algorithm AFP does not guarantee to catch a global maximum, the results are typically very good and the Lebesgue constant of the computed points turns out to be (much) lower than the upper bound (18). On the other hand, the Approximate Fekete Points are asymptotically optimal in some sense, since it has been proved that the associated discrete uniform probability measure (the measure with equal weights $1/N$ at the mass points $\{\xi_{i_k}\}$) converges weakly to the pluripotential theoretic equilibrium measure of the compact set K; cf. [4].

3.1 Numerical examples

We'll now apply Algorithm AFP to the extraction of Approximate Fekete Points $\tilde{\mathcal{F}}_n$ from the norming grids $X_n = \widehat{G}_{kn}$ on a spherical triangle $\mathcal{T}$, that in view of Proposition 1 form a polynomial mesh. Such an algorithm has been implemented in Matlab, adapting some routines of the recent package dCATCH in [12] to spherical polynomial spaces.

In order to construct the extraction mesh, we have chosen as maximum allowed circumradius $\sin(\omega^*) = \sin(\pi/5) \approx 0.587$, otherwise the spherical triangle is iteratively splitted into smaller ones by the side midpoints until all circumradii do not exceed $\sin(\pi/5)$, and the mesh is obtained by union of the corresponding Chebyshev-Dubiner grids. We recall that the mesh constant c is then the maximum of the single grid constants $c_k(\omega^*)$ (cf. [8]). Since $\alpha(\omega^*) \le \alpha(\pi/5) \approx 1.6$, we can take for example $k = 7$, obtaing a polynomial mesh constant $c \le c_7(\pi/5) = 1/\cos(2\pi\alpha(\pi/5)/7) \approx 7.4$.

We stress that a choice like $\max \omega^* = \pi/5$ is a trade-off between the need of avoiding too large mesh constants with ω^* close to $\pi/4$, in view of (18) (which however as we shall see is by large an overstimate), and the need of avoiding too

many triangles (small ω^*), in order to control the mesh cardinality that impacts directly the computational cost. Notice that $\omega^* = \pi/5$ corresponds to a quite large spherical triangle: by suitably rotating the circumcenter at the north pole, the cap base circle is the 54th parallel north in a geographical perspective, that is to fix ideas a cap containing all Scandinavia, Alaska, Greenland, and a large portion of northern Canada and Siberia.

For the numerical tests we have chosen a large spherical triangle, namely the octant with vertices $(1,0,0)$,(0,1,0), $(0,0,1)$. Since in this case the circumcenter is $(1/3,1/3,1/3)$ and the circumradius is $|(1,0,0)-(1/3,1/3,1/3)| = \sqrt{1-1/3} > \sin(\pi/5)$, the octant is automatically splitted into four triangles with circumradii not exceeding $\sin(\pi/5)$ and the polynomial mesh constructed by union. In Fig. 8 we have plotted the Lebesgue constant of interpolation at the $(n+1)^2$ Approximate Fekete Points extracted from the polynomial mesh described above, for degree $n = 1,2,\ldots,15$. For the purpose of comparison, we have also displayed the Lebesgue constant of hyperinterpolation (that is the uniform norm of the hyperinterpolation operator), recently implemented via a near-algebraic quadrature formula on spherical triangles; cf. [22]. Notice that the actual values of the interpolation Lebesgue constant are much smaller than the upper bound 8 (here $X_n = \widehat{G}_{7n}$), which increases quadratically in the degree.

We recall that to hyperinterpolate at degree n one needs a quadrature formula exact at degree $2n$, indeed we have used $(2n+1)^2$ Tchakaloff quadrature points, that can be computed by the compression algorithm described in [21]. From this point of view, interpolation at Approximate Fekete Points is more convenient than hyperinterpolation at Tchakaloff Points, since the Lebesgue constant turns out to be of lower size (less that 2/3 on average) and the number of points is roughly 1/4 when n increases.

The comparison is more clear if we consider some examples of function reconstruction. We have taken the following six test functions with different regularity from the numerical tests of [22]:

$$f_1(x,y,z) = 1+x+y^2+x^2y+x^4+y^5+x^2y^2z^2\ ,\quad f_2(x,y,z) = \cos(10(x+y+z))\ ,$$

$$f_3(x,y,z) = \exp\left(-|\mathcal{P}-\mathcal{P}_0|^2\right)\ ,\quad f_4(x,y,z) = \exp\left(-|\mathcal{P}-\mathcal{Q}_0|^2\right)$$

$$f_5(x,y,z) = |\mathcal{P}-\mathcal{P}_0|^5\ ,\quad f_6(x,y,z) = |\mathcal{P}-\mathcal{Q}_0|^5\ ,$$

where $\mathcal{P} = (x,y,z)$, $\mathcal{P}_0 = (0,0,1)$ is the north pole, a vertex of the octant, and $\mathcal{Q}_0 = (\frac{1}{\sqrt{3}},\frac{1}{\sqrt{3}},\frac{1}{\sqrt{3}})$ is the centroid. In particular, f_1 is a polynomial of degree 6, f_2, f_3 and f_4 are smooth, while f_5 and f_6 are C^4 with a singularity of the 5th derivatives at $\mathcal{P}_0$ and $\mathcal{Q}_0$.

The numerical results are reported in Fig. 9, where we have displayed the relative L^2-errors computed by a Tchakaloff-like quadrature formula of exactness degree 40 as in [22]. Observe that, as expected, the error on f_1 falls down around machine precision for $n \geq 6$, and the convergence is slower for the less regular functions f_5 and f_6. Moreover, the interpolation and hyperinterpolation errors are quite close with respect to the approximation degree, whereas interpolation converges more rapidly with respect to the sampling cardinality.

On the base of these and several other numerical tests with spherical triangles of different size and functions of different regularity, we are confident that the proposed method, namely the construction of polynomial meshes by Chebyshev-Dubiner norming grids and the subsequent extraction of Approximate Fekete Points by basic numerical linear algebra routines, provides a reasonably efficient, flexible and stable approach for polynomial approximation of moderate degree on spherical triangles. In particular, we may consider the present work as a starting step towards global polynomial modelling on more complicated regions such as spherical polygons, for example in a geomathematical perspective.

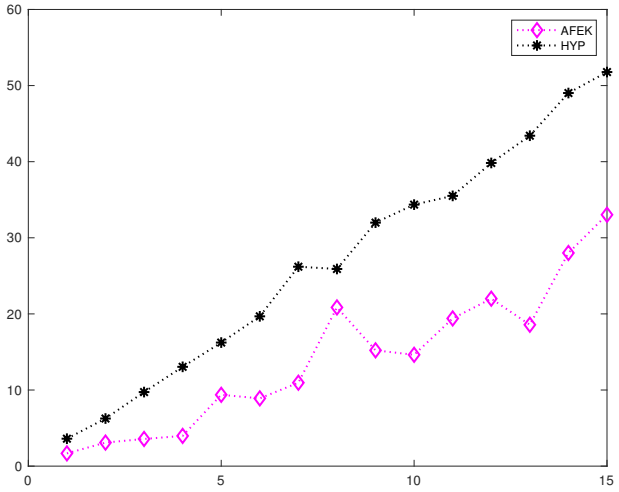

Figure 8: Lebesgue constants of interpolation at Approximate Fekete Points and hyperinterpolation at Tchakaloff Points on a spherical octant for degree $n = 1, 2, \ldots, 15$.

References

[1] C. An, X. Chen, I.H. Sloan and R. Womersley, Well conditioned spherical designs for integration and interpolation on the two-sphere, SIAM J. Numer. Anal. 48 (2010), 2135–2157.

[2] V. Baramidze, M.J. Lai and C.K. Shum, Spherical splines for data interpolation and fitting, SIAM J. Sci. Comput. 28 (2006), 241–259.

[3] L. Bos, A Simple Recipe for Modelling a d-cube by Lissajous curves, Dolomites Res. Notes Approx. DRNA 10 (2017), 1–4.

[4] L. Bos, J.-P. Calvi, N. Levenberg, A. Sommariva and M. Vianello, Geometric Weakly Admissible Meshes, Discrete Least Squares Approximations and Approximate Fekete Points, Math. Comp. 80 (2011), 1601–1621.

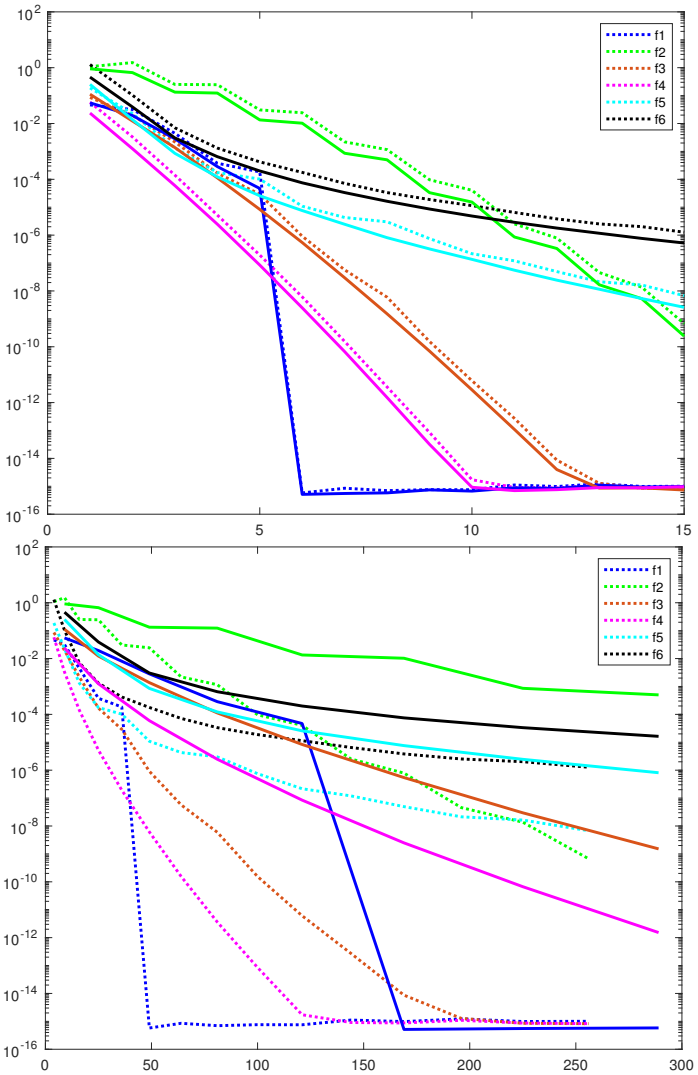

Figure 9: Relative L^2 reconstruction errors on a spherical octant for the six test functions with respect to the degree n (top) and the sampling cardinality (bottom) by interpolation at Approximate Fekete Points (dotted lines) and hyperinterpolation at Tchakaloff Points (solid lines).

[5] L. Bos, S. De Marchi, A. Sommariva and M. Vianello, Computing multivariate Fekete and Leja points by numerical linear algebra, SIAM J. Numer. Anal. 48 (2010), 1984–1999.

[6] L. Bos, N. Levenberg and S. Waldron, Pseudometrics, distances and multivariate polynomial inequalities, J. Approx. Theory 153 (2008), 80–96.

[7] L. Bos and M. Vianello, Low cardinality admissible meshes on quadrangles, triangles and disks, Math. Inequal. Appl. 15 (2012), 229–235.

[8] J.P. Calvi and N. Levenberg, Uniform approximation by discrete least squares polynomials, J. Approx. Theory 152 (2008), 82–100.

[9] M.F. Carfora, Interpolation on spherical geodesic grids: A comparative study, J. Comput. Appl. Math. 210 (2007), 99–105.

[10] W. zu Castell, N. Lain Fernandez and Y. Xu, Polynomial interpolation on the unit sphere. II, Adv. Comput. Math. 26 (2007), 155–171.

[11] A. Civril and M. Magdon-Ismail, On Selecting a Maximum Volume Submatrix of a Matrix and Related Problems, Theor. Comput. Sci. 410 (2009), 4801–4811.

[12] M. Dessole, F. Marcuzzi, A. Sommariva and M. Vianello, dCATCH: numerical package for d-variate polynomial fitting (2020).
`https://www.math.unipd.it/~marcov/dCATCH.html`

[13] M. Dubiner, The theory of multidimensional polynomial approximation, J.Anal. Math. 67 (1995), 39–116.

[14] W. Freeden, Z.M. Nashed and M. Schreiner, Spherical Sampling, Birkhäuser, Cham, 2018.

[15] M. Gentile, A. Sommariva and M. Vianello, Polynomial approximation and quadrature on geographic rectangles, Appl. Math. Comput. 297 (2017), 159–179.

[16] A. Kroó, On optimal polynomial meshes, J. Approx. Theory 163 (2011), 1107–1124.

[17] F. Piazzon and M. Vianello, Markov inequalities, Dubiner distance, norming meshes and polynomial optimization on convex bodies, Optim. Lett.13 (2019), 1325–1343.

[18] R.J. Renka, Algorithm 623: Interpolation on the surface of a sphere, ACM Trans. Math. Software 10 (1984), 437–439.

[19] I.H. Sloan and R.S. Womersley, How Good can Polynomial Interpolation on the Sphere be?, Adv. Comput. Math. 14 (2001), 195–226.

[20] A. Sommariva and M. Vianello, Computing approximate Fekete points by QR factorizations of Vandermonde matrices, Comput. Math. Appl. 57 (2009), 1324–1336.

[21] A. Sommariva and M. Vianello, Near-algebraic Tchakaloff-like quadrature on spherical triangles, preprint, 2021.
`https://www.math.unipd.it/~marcov/pdf/spheretri.pdf`

[22] A. Sommariva and M. Vianello, Numerical hyperinterpolation over spherical triangles, preprint, 2021.
https://www.math.unipd.it/~marcov/pdf/hyp3sph.pdf

[23] A. Sommariva and M. Vianello, Software package for polynomial interpolation on spherical triangles, alpha version, February 2021.
https://www.math.unipd.it/~marcov/alvise/software.html

[24] J. Stillwell, The Four Pillars of Geometry, Springer, New York, 2005.

[25] M. Vianello, Subperiodic Dubiner distance, norming meshes and trigonometric polynomial optimization, Optim. Lett. 12 (2018), 1659–1667.

[26] M. Vianello, Chebyshev-Dubiner norming webs on starlike polygons, J. Inequal. Spec. Funct. 10-3 (2019), 26–32.

[27] Y. Xu, Polynomial interpolation on the unit sphere, SIAM J. Numer. Anal. 41 (2003) 751–766.